Korean J. Chem. Eng., 32(4), 597-608 (2015)
DOI: 10.1007/s11814-014-0207-z

pISSN: 0256-1115
eISSN: 1975-7220

Dynamic modeling and control of industrial crude terephthalic acid hydropurification process

Zhi Li, Weimin Zhong†, Yang Liu, Na Luo, and Feng Qian†

Key Laboratory of Advanced Control and Optimization for Chemical Processes, Ministry of Education, East China University of Science and Technology, Shanghai 200237, China
(*Received 4 March 2014 • accepted 22 July 2014*)

Abstract−Purified terephthalic acid (PTA) is critical to the development of the polyester industry. PTA production consists of *p*-xylene oxidation reaction and crude terephthalic acid (CTA) hydropurification. The hydropurification process is necessary to eliminate 4-carboxybenzaldehyde (4-CBA), which is a harmful byproduct of the oxidation reaction process. Based on the dynamic model of the hydropurification process, two control systems are studied using Aspen Dynamics. The first system is the ratio control system, in which the mass flows of CTA and deionized water are controlled. The second system is the multivariable predictive control-proportional-integral-derivative cascade control strategy, in which the concentrations of 4-CBA and carbon monoxide are chosen as control variables and the reaction temperature and hydrogen flow are selected as manipulated variables. A detailed dynamic behavior is investigated through simulation. Results show that the developed control strategies exhibit good control performances, thereby providing theoretical guidance for advanced control of industry-scale PTA production.

Keywords: Terephthalic Acid, Hydropurification Reaction, Dynamic Modeling, Multivariable Predictive Control, DMC Plus

INTRODUCTION

Pure terephthalic acid (PTA), which is one of the most important petrochemical products, is the main raw material of polyesters, which are widely used in textile and packaging industries. In PTA production, terephthalic acid (TA) is usually produced by the homogeneous liquid-phase oxidation of *p*-xylene with air or molecular oxygen in acetic acid within the temperature range of 190 °C to 200 °C and in the presence of cobalt acetate and manganese acetate catalysts with bromide[1-3].

However, the byproduct of the outlet includes 4-carboxybenzaldehyde (4-CBA), which is the main impurity. Considered chemically and physically similar to TA, 4-CBA is one of the most difficult contaminants to remove in the separation process and it causes the discoloration of TA and decreases both the average molecular weight of the polymer and the rate of polymerization in polyester production [4,5]. Crude TA (CTA) is a product of the *p*-xylene oxidation reaction process that has high 4-CBA content. Thus, a purification process is needed to decrease the 4-CBA content. In the current hydropurification process, CTA is purified by hydrogenation in deionized water at 270 °C to 290 °C under high pressure with carbon-coated palladium (Pd/C) catalyst [6]. The product of this process contains a tiny fraction of 4-CBA that can induce negligible effect on the polyester production.

The hydropurification process is evidently essential to PTA production. Myerson et al. [7-9] studied the aging of PTA for many years. Shaogang et al. [10] explored the mass transfer characteristics of the fixed-bed reactor for hydro-refining of TA and developed a steady-state heterogeneous 1D model of the reactor, in which the transport phenomenon by plug flow in the axial direction was considered. Azarpour et al. [6] invented a fully dynamic fixed-bed reactor model along with a deactivation model of Pd/C catalyst for the industrial trickle bed reactor of PTA production plant. This fully dynamic reactor can predict the concentration profiles of the reaction components and the trend of the Pd/C catalyst deactivation. Moreover, the reactor can be used any time for the catalyst deactivation and operational condition analysis. Weimin et al. [11,12] simulated the CTA hydro-treating reaction and proposed a dynamic model of the PTA hydrogenation reaction process based on Aspen Plus and Aspen Dynamics. Unlike *p*-xylene oxidation and solvent recycle processes, studies on CTA hydropurification process are limited, particularly on the dynamics and control structure [13-19]. The PTA industry is significantly growing, especially in the last 10 years. Dynamic simulation and optimal control have become a major issue in thevPTA industry because of the increasing pressures caused by the global market competition.

Proportional-integral-derivative (PID) controllers are important in the process control of the PTA industry because of their control performance, simplicity, and technology maturity. These controllers, however, have limitations in more complex system applications and are tuned without considering the constraints of input signal processing [20,21]. For coupled systems, achieving satisfactory performance by PID controllers is difficult because of the many risks encountered. In addition, direct designing and performing advanced control schemes in industrial plants are expensive. Satisfactory control performance of advanced control systems can eas-

†To whom correspondence should be addressed.
E-mail: wmzhong@ecust.edu.cn, fqian@ecust.edu.cn

ily be achieved with the development of computer technology and control theory, such as multivariable predictive control (MPC) strategy, which can remedy some of the deficiencies of the PID controller. Richalet et al. [22] first introduced the model predictive heuristic control in 1978, followed by the dynamic matrix control (DMC) and then generalized predictive control [23]. The DMC algorithm was developed by Shell Oil, who successfully implemented some practical applications [24-26]. The DMC algorithm can handle constraints imposed on the controlled/manipulated variables. In the CTA hydropurification process, the 4-CBA content in the product is sensitive to the changes in hydrogen flow load, reaction temperature, and the density of feed CTA. In practical plants, the density of feed CTA is controlled by two single-loop PID controllers. It is necessary to develop a new strategy to handle the balance between CTA and deionized water. Studies on the dynamic modeling and control strategies of the CTA hydropurification process are significantly relevant.

We describe here a dynamic model of hydropurification process [12]. The stability and accuracy of the model are improved, as introduced in Section 2, by adopting the dynamic modeling procedure proposed by Luyben et al. [24-26]. A double closed loop ratio control system and a DMC-PID cascade control strategy are developed based on the model of Aspen Dynamics and DMC plus, as presented in Section 3. Both controllers can accomplish the control demands. Compared with the PID controller, these two controllers exhibit good dynamic responses. The conclusions of this study are cited in Section 4.

INDUSTRIAL HYDROPURIFICATION PROCESS AND DYNAMIC MODELING

1. Industrial Catalytic Hydrogenation Reaction Process

The interim product CTA from *p*-xylene oxidation reaction process has approximately $2{,}500\times10^{-6}$ (mass percentage) of 4-CBA. The molecular structure of 4-CBA is similar to TA and, thus, these two compounds can easily form a eutectic system. Separating 4-CBA from TA is difficult by conventional physical methods. The purification process is performed after the *p*-xylene oxidation process. In this study, approximately 37% of CTA (mass percentage) was heated together with the deionized water to about 285 °C through five successive pre-heaters in the plant. The completely dissolved CTA solution and an excessive flow of high-pressure hydrogen gas were subsequently injected into the top of the fixed-bed hydrogenation reactor and passed through the catalyst bed, in which the 4-CBA was hydrogenated to *p*-toluic (PT) acid. The product of hydrogenation reaction, i.e., PTA, was separated from PT acid and other small quantities of impurities via crystallization and centrifugation units. The final PTA product contains $<25\times10^{-6}$ of 4-CBA (mass percentage).

4-CBA undergoes complex reactions in the purification process, during which the hydrogenation reaction is completed with a decarbonylation process [27,28]. The CO produced during decarbonylation is harmful to Pd/C catalyst. The following reactions are considered in the 4-CBA hydrogenation process in the catalytic bed of the reactor:

Eq. (1) is the main hydrogenation reaction and Eq. (2) is the side decarbonylation reaction [2,10,27].

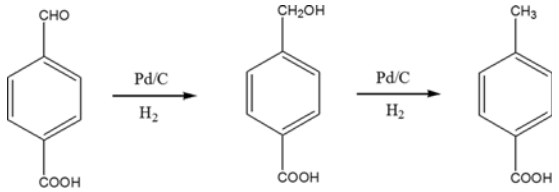

(1)

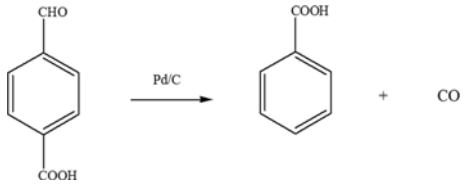

(2)

The kinetics of the reactions are shown below; Eqs. (3) to (5) correspond to the main reaction, whereas Eqs. (6) and (7) conform to the side reaction [10,27,28].

$$-\frac{dc_{4-CBA}}{dt}=k_{01}e^{-\frac{E1}{RT}}C_{4-CBA}^{n1}C_{H_2}^{n2} \tag{3}$$

$$\frac{dc_{4-HMBA}}{dt}=k_{01}e^{-\frac{E1}{RT}}C_{4-CBA}^{n1}C_{H_2}^{n2}-k_{02}e^{-\frac{E2}{RT}}C_{4-HMBA}^{n3}C_{H_2}^{n4} \tag{4}$$

$$\frac{dc_{PT-acid}}{dt}=k_{02}e^{-\frac{E2}{RT}}C_{4-HMBA}^{n3}C_{H_2}^{n4} \tag{5}$$

$$-\frac{dc_{4-CBA}}{dt}=k_{03}e^{-\frac{E_3}{RT}}C_{4-CBA}^{n5} \tag{6}$$

$$\frac{dc_{BA}}{dt}=k_{03}e^{-\frac{E_3}{RT}}C_{4-CBA}^{n5} \tag{7}$$

2. Dynamic Model of Hydropurification Process

A dynamic model of the hydropurification process, which contains pre-heaters, reactor, and crystallizers, is established using the Aspen Dynamics based on the steady model using Aspen Plus in accordance with a previous study [12]. The coupled heat and mass balances are investigated in the pre-heaters and crystallizers, in which Eqs. (3) to (7) are considered in the reactor. The pressure-driven approach is selected in the Aspen Dynamics environment. The sizes of the heat exchangers, reactor, and crystallizers are then set according to the measurements in the actual industrial plant, and conventional controllers are added. The flowchart of hydropurification process is shown in Fig. 1, and the diagram of the dynamic model of the process is shown in Fig. 2. The slurry containing CTA and deionized water is injected to the fixed-bed hydrogenation reactor after it is heated to 270 °C to 290 °C via the five pre-heaters. The CTA is subsequently purified in water by hydrogenation over the Pd/C catalyst in the reactor to convert 4-CBA to PTA. Once the conversion is completed, the PTA is separated from the slurry through crystallization.

The difference between the model in [12] and the model in this study is that the kinetic data of the reactions shown in Table 1 are re-adjusted to calibrate the model after conducting a series of simulations on steady state based on plant data. The actual plant and simulation data obtained using the kinetic data of this study and the reference data are shown in Fig. 3. Controller parameters are reset according to the Tyreus-Luyben method [29], resulting in bet-

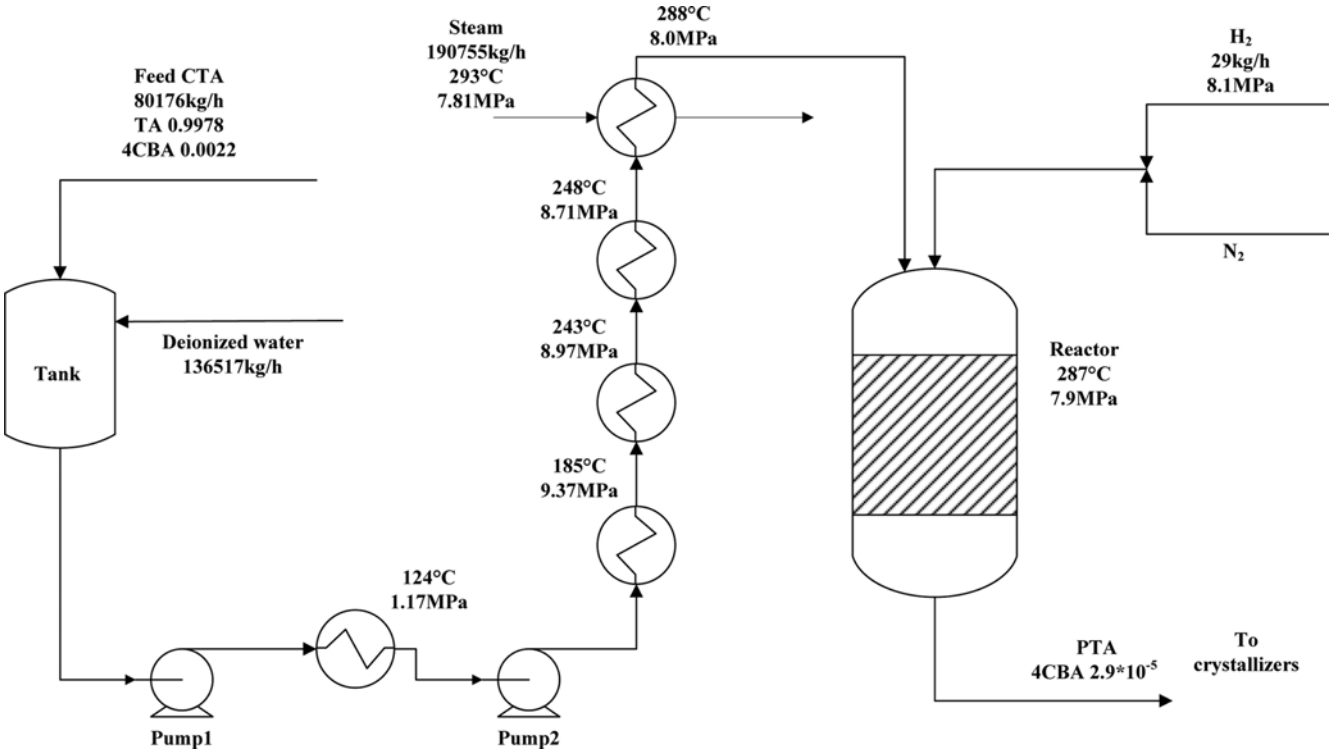

Fig. 1. Flowchart of industrial CTA hydropurification process.

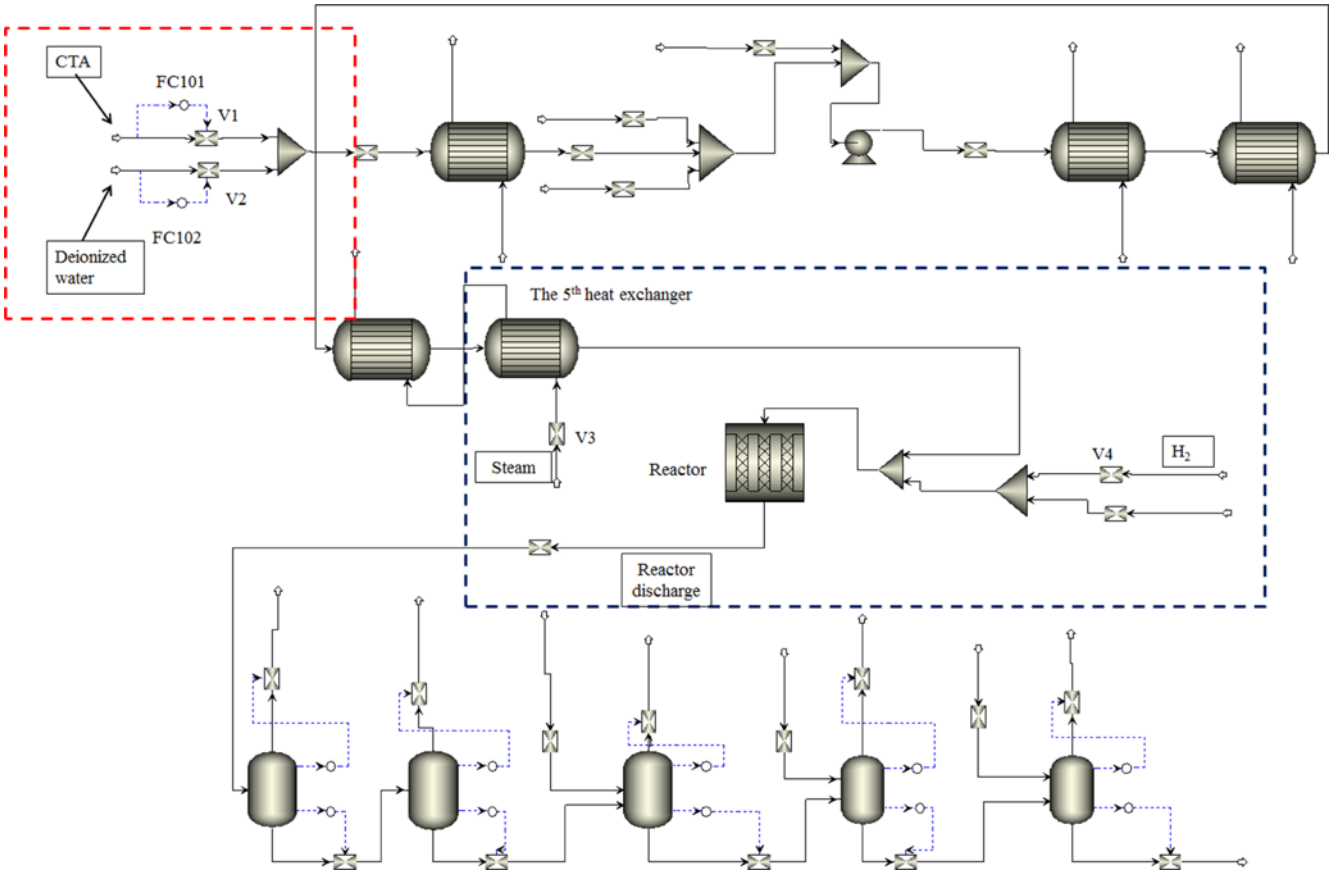

Fig. 2. Dynamic model of industrial CTA hydropurification process.

Table 1. Kinect data of the reactions

Item	Data in reference [12]	Data in this study
Frequency factor	k_{01}=0.67	k_{01}=0.88
	k_{02}=0.2558	k_{02}=0.5971
	k_{03}=69	k_{03}=68
Reaction order	n_1=0.98, n_2=0.26, n_3=0.70, n_4=0.60, n_5=0.30	
Activation energy	E_1=18.66 kJ/mol, E_2=28.04 kJ/mol, E_3=724.143 kJ/mol	

ter control performance. Some of the refluxes are cut off, compelling the process model to be clearer and more stable. The most crucial improvement is that two advanced control strategies are proposed, as discussed in the following section.

CONTROL OF INDUSTRIAL HYDROPURIFICATION PROCESS

The industrial hydrogenation process has many control loops, in which the majority of them are single-control loops (e.g., CTA feed, deionized water feed, hydrogen flow, reactant feed temperature, and reactor pressure controls). The hydrogenation process generally aims to reduce the concentration of 4-CBA and to purify CTA. The reactor is the most important unit of the process.

After the dynamic model of the hydrogenation process is developed, as presented in Section 2.2, the control degrees of freedom are analyzed. The flows of 4-CBA and CO in the product are related to the production quality; thus, they are selected as the controlled variables (CV). The reactor has three control degrees of freedom, namely, reactor temperature, flow of feed CTA, and H_2 flow; these

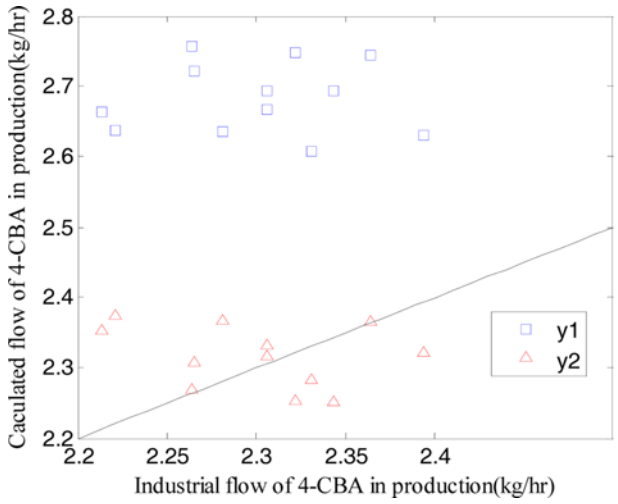

Fig. 3. Comparison of industrial flow of 4-CBA in production with model predictions (y1 is the result using kinetic data in reference; y2 is the result using kinetic data in Table 1).

elements can be used to control the two CVs. The flow of feed CTA follows the plan and schedule of the plant. Accordingly, the reactor temperature and the H_2 flow are selected as the manipulated variables (MVs) of the reactor. Two control systems, feed and reactor control systems, are examined in this study via the Aspen Dynamics.

1. Feed Control Using Double Closed-loop Ratio Control System

The CTA slurry concentration in the production process needs to be maintained at a constant value; the slurry with higher concentration of CTA may crush the catalyst bed in the reactor, which then may lead to an accident. By contrast, lower concentration of

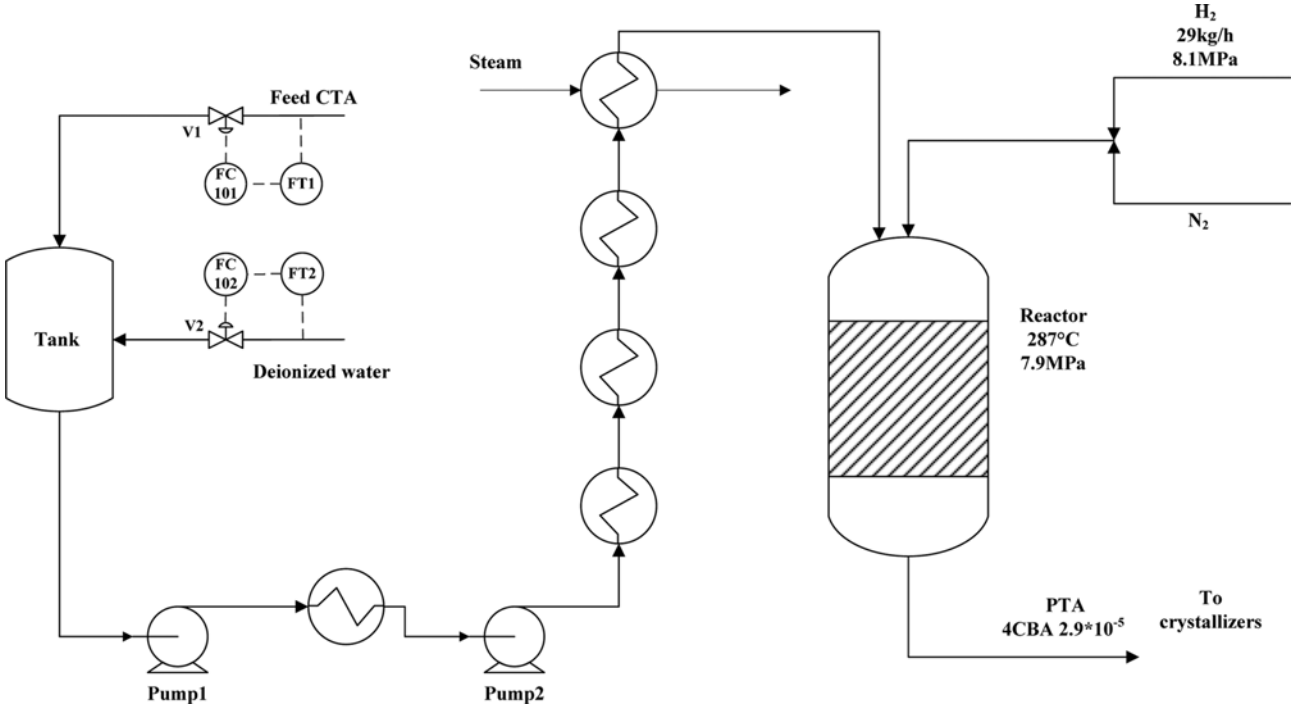

Fig. 4. Control structure of CS1.

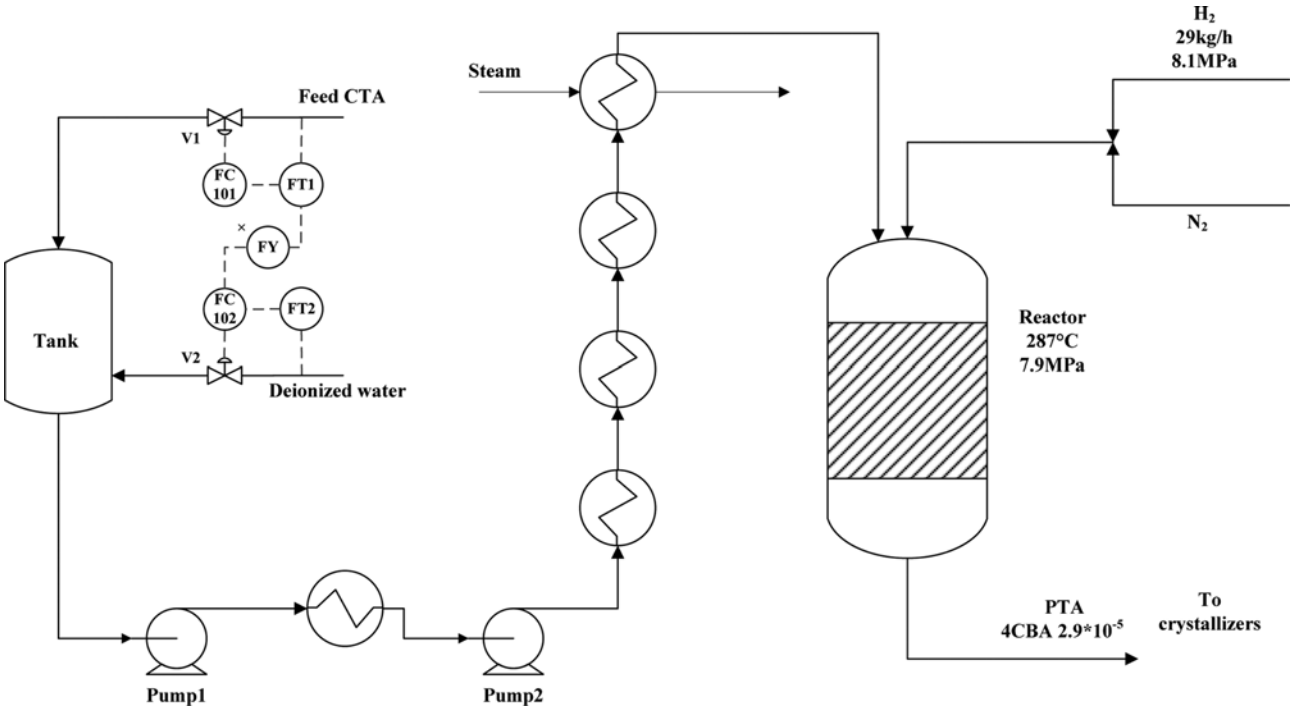

Fig. 5. Control structure of CS2.

CTA affects the reaction efficiency. In the actual process, two single control loops are used to control the feed flows of the CTA and deionized water. When the plan and schedule of the plant change, the setpoint of the flow of CTA is increased or reduced accordingly. At the same time, the setpoint of the flow of deionized water must be adjusted to maintain the concentration of the slurry constant. However, the setpoint of the flow controller is manually adjusted. In this case, the flow of deionized water cannot be easily changed based on the change of feed CTA flow in time. Thus, a double closed-loop ratio control strategy is developed.

1-1. Case Study 1 (CS1)

The control structures used in the industrial process for this case are shown in Fig. 4. The mass flow of CTA is controlled by controller FC101, whose setpoint is 80176 kg/hr via valve V1, and the mass flow of deionized water is controlled by controller FC102, whose setpoint is 136515 kg/hr. Both of the two controllers are PI and tuned via the relay feedback test with Tyreus-Luyben settings in Aspen Dynamics [29]. The concentration of CTA slurry is maintained at 37% by the two separate controllers.

1-2. Case Study 2 (CS2)

In this case, a double closed-loop ratio control structure is designed (Fig. 5). The feed flow of CTA is chosen as the active variable and the flow of deionized water is selected as the passive one. When the active variable changes, the passive variable changes as well. The control structure in CS1 remains the same, but the mode of FC102 is switched from auto to cascade. A multiply is added to achieve steady ratio. The input of the multiply is the setpoint of FC101 and the output is the SPRemote of FC102.

1-3. Dynamic Responses

The responses of the two control structures, CS1 and CS2, are obtained for principal changes. A ±5 mass% step change in the feed flow of CTA is considered the principal change in the load requirements. Fig. 6(a) shows the dynamic response of CS1. When the load is increased by 5%, the setpoint of the feed flow of CTA changes from 80,176 kg/hr to 84,184.8 kg/hr, and the process value gradually increases to 84,184.8 kg/hr by the controller FC101 via valve V1. This simulation, however, is pressure driven and the pressure of Mix1 remains constant. Thus, the flow of deionized water rapidly drops to 135,708 kg/h and then increases up to 136,517 kg/hr by the controller FC102 via valve V2. Meanwhile, the CTA slurry concentration increases to 38.14% and vice versa. The simulation shows that this kind of control structure cannot maintain a constant concentration. When a disturbance in the flow of CTA occurs or the load is changed, the setpoint of the controller FC102 must be reset to ensure that the concentration does not change. Fig. 6(b) shows the dynamic response of CS2. When the load is increased by 5%, the flow of feed CTA response is the same as in the case of CS1, whereas the flow of deionized water, which is different from CS1, gradually increases to 136,517 kg/hr. The CTA slurry concentration evidently holds the line. The results of the simulation demonstrate that the double closed-loop ratio control structure can maintain a constant concentration, effectively reducing the workload of the operator, and ensuring the safety of the process.

2. Reactor Control Using DMC-PID Cascade Control Strategy

The purpose of the control of the reactor is to ensure that the concentrations of 4-CBA and CO in the flow of the product are within a certain range to guarantee product quality. At the same time, the two MVs must also be controlled within a certain range to maintain a stable and efficient reaction. However, during the CTA hydrogenation reaction, the reaction temperature, hydrogen flow, and concentrations of 4-CBA and CO are coupled with large correlation. The reaction temperature or hydrogen flow can affect the

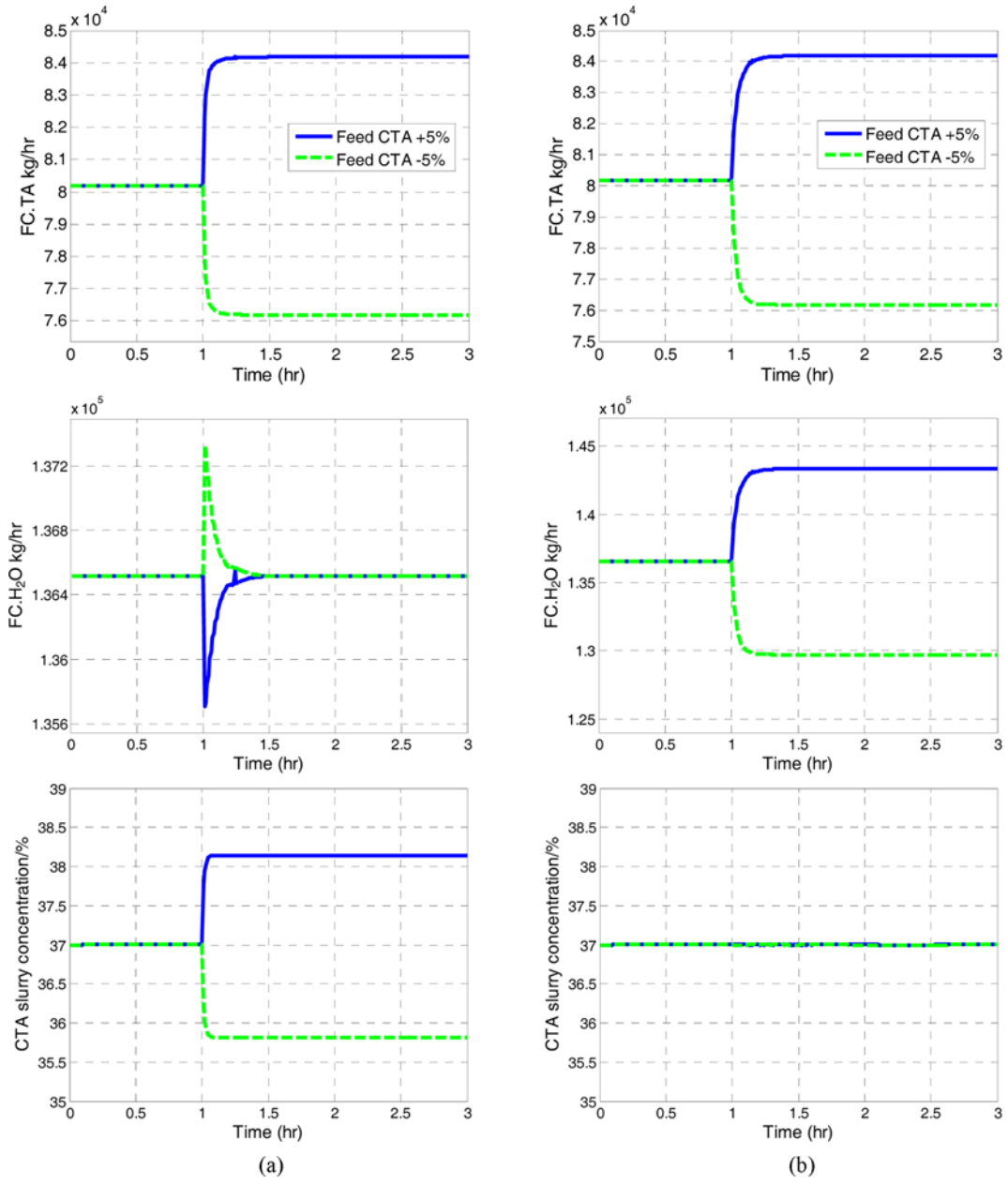

Fig. 6. (a) Dynamic responses of CS1. (b) Dynamic responses of CS2.

concentrations of 4-CBA and CO. The sensitivity analysis of the process based on the steady state, shown in Fig. 7, demonstrates that when the H_2 flow increases, both the flows of 4-CBA and CO in the product decrease. When the reaction temperature increases, the flow of 4-CBA in the product decreases, whereas the flow of CO increases.

The single-loop control systems applied in industrial processes are barely satisfactory when dealing with the multi-input and multi-output problem. To solve this problem, we analyzed the exploratory research of a DMC-PID cascade control system based on the dynamic mechanism model. The following two case studies discuss the described control systems. In particular, the feed control system of the two case studies is the double closed-loop ratio control system, which is used in CS2.

2-1. Case Study 3 (CS3)

The single-loop control system applied in the industrial process is used in this case (Fig. 8). Two control loops are involved. First, the reaction temperature is manipulated by the cold side outlet temperature of the fifth heat exchanger. The temperature of the hot side inlet steam and the efficiency of the heat exchanger are assumed constant to facilitate this study. Thus, the cold side outlet temperature is controlled by the flow of Steam. TC101 is a PI controller and tuned via the relay feedback test with the Tyreus-Luyben settings, similar to the case in CS1. When the temperature drifts, the controller TC101 can control the flow of steam through valve V3. Second, the flow of hydrogen is controlled by controller FC103, which is also tuned via the relay feedback test with the Tyreus-Luyben settings.

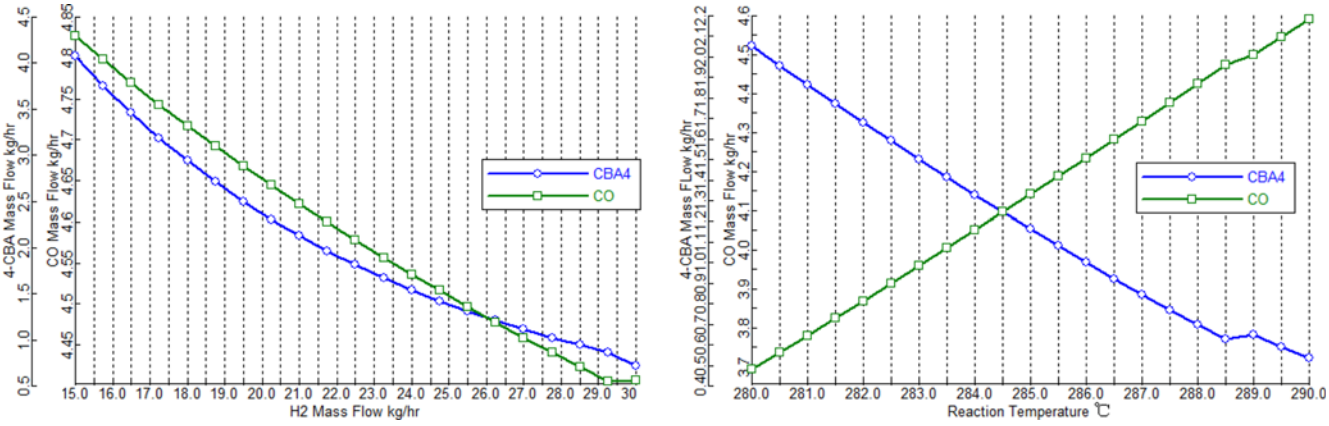

Fig. 7. Sensitivity analysis of CTA hydrogenation reaction based on the steady-state model.

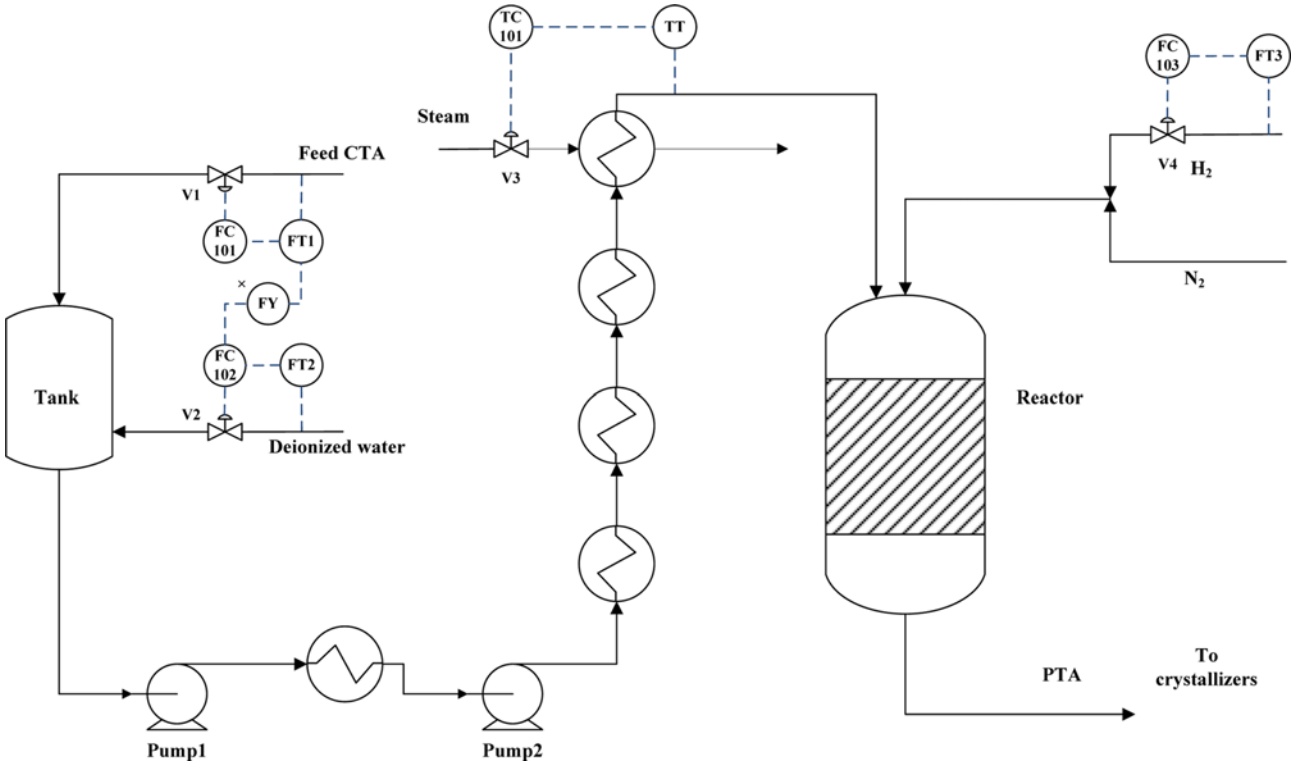

Fig. 8. Control structure of CS3.

Table 2. Range of the MVs and CVs

	Description	Maximum variation
CV_1	Reactor discharge flow of CO	5 kg/hr to 5.4 kg/hr
CV_2	Reactor discharge flow of 4-CBA	2.2 kg/hr to 2.4 kg/hr
MV_1	Temperature of feed before entering the reactor (TC101.SP)	280 °C to 290 °C
MV_2	H_2 flow (FC103.SP)	15 kg/h to 30 kg/h

2-2. Case Study 4 (CS4)

In this case, a DMC-PID cascade control strategy is designed to achieve the following objectives: (1) ensure the product quality (maintain the CVs within a certain range) and (2) maintain the reaction in normal condition (MVs must also be restricted within a certain range).

The constraints of the CVs and MVs are identified using Aspen DMCplus (Table 2). The first step in implementing DMCplus is to model the process based on Aspen Dynamics; the model is obtained by collecting the data of the dynamic model while perturb-

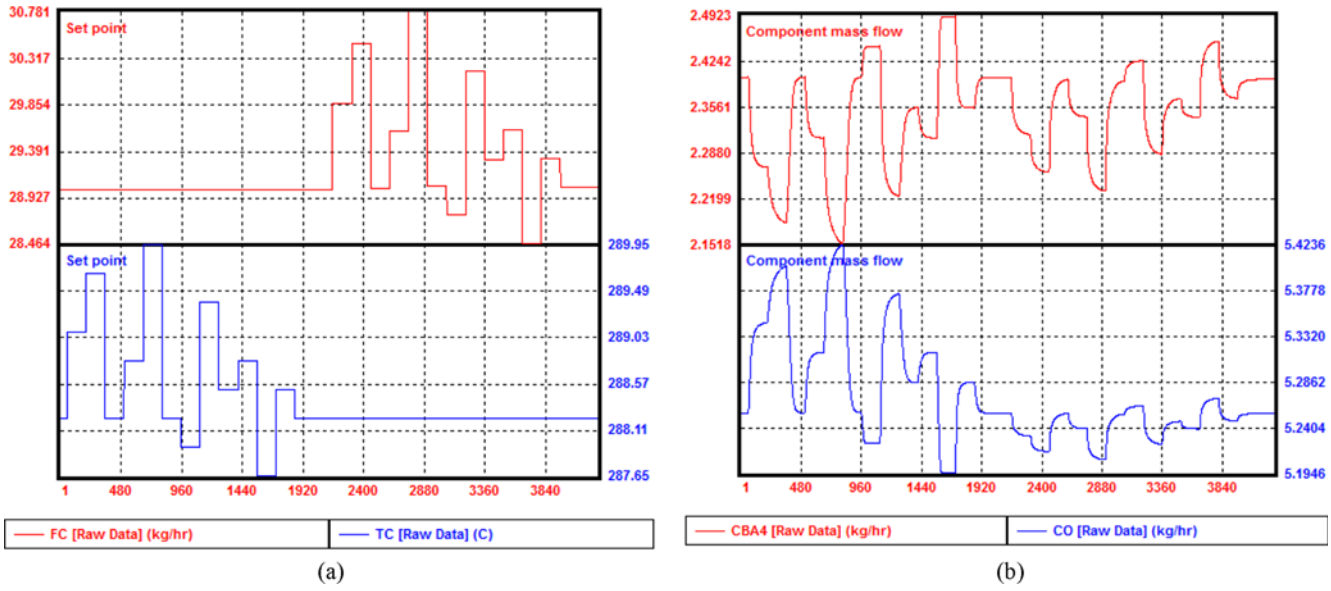

Fig. 9. (a) Step changes of MV1 and MV2. (b) Dynamic responses of CV1 and CV2.

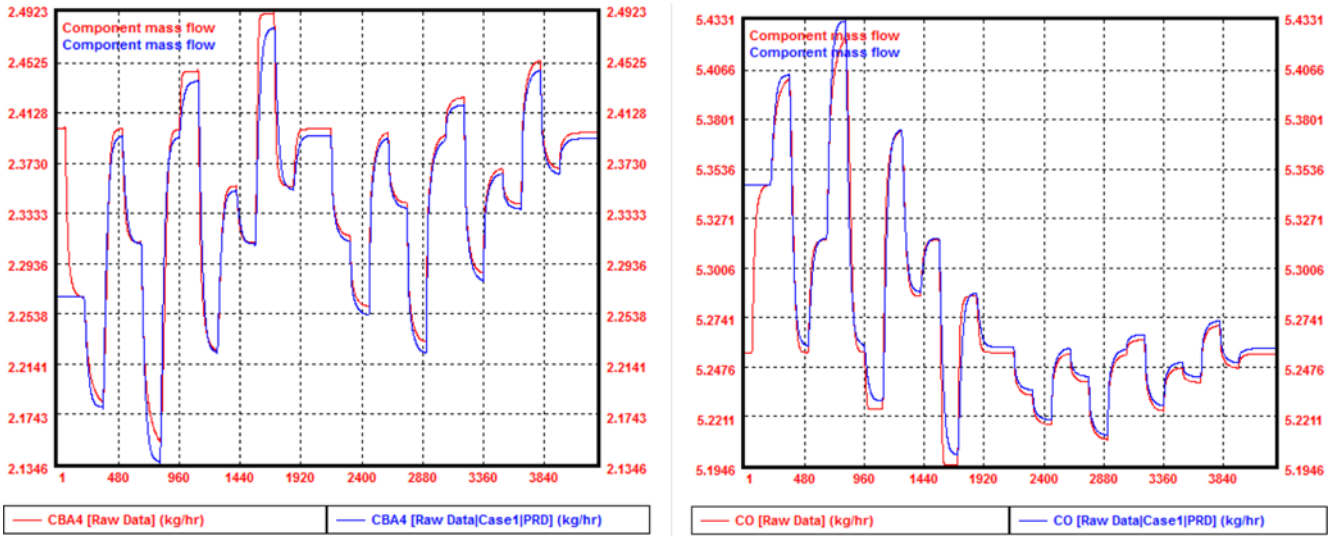

Fig. 10. Actual and model identification results of 4-CBA and CO.

ing them [30]. A series of manipulated variables step response are tested on the open-loop conditions based on Aspen Dynamics to design a proper DMC controller. Fig. 9(a) shows the step changes of MV1 and MV2; the first duration (36 h) is the setpoint of feed temperature step changes and the rest is the setpoint of H_2 flow changes. The dynamic responses of the flows of 4-CBA and CO outputs are shown in Fig. 9(b). The DMCplus software is compatible with two identification methods: the FIR and subspace identification models. In this study, the FIR identification method is used to identify the model. After the transient time to steady state, the number of coefficients and a smoothing factor are satisfied. The prediction results of the CVs and the results of model identification are shown in Fig. 10.

The developed DMC controller is applied to the control system. The control structure (Fig. 12) is adjusted from CS3. The input signals of the DMC controller are the reactro discharge flow of 4-CBA and CO, and the outputs of the DMC controller are the set points

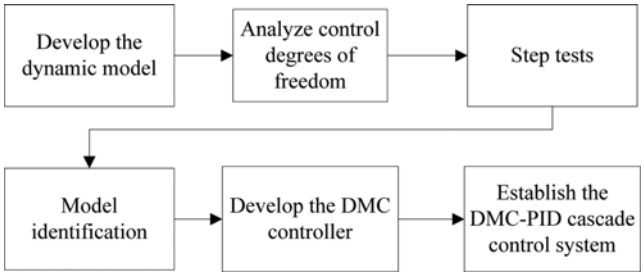

Fig. 11. Flowchart of the development of the DMC-PID cascade control system.

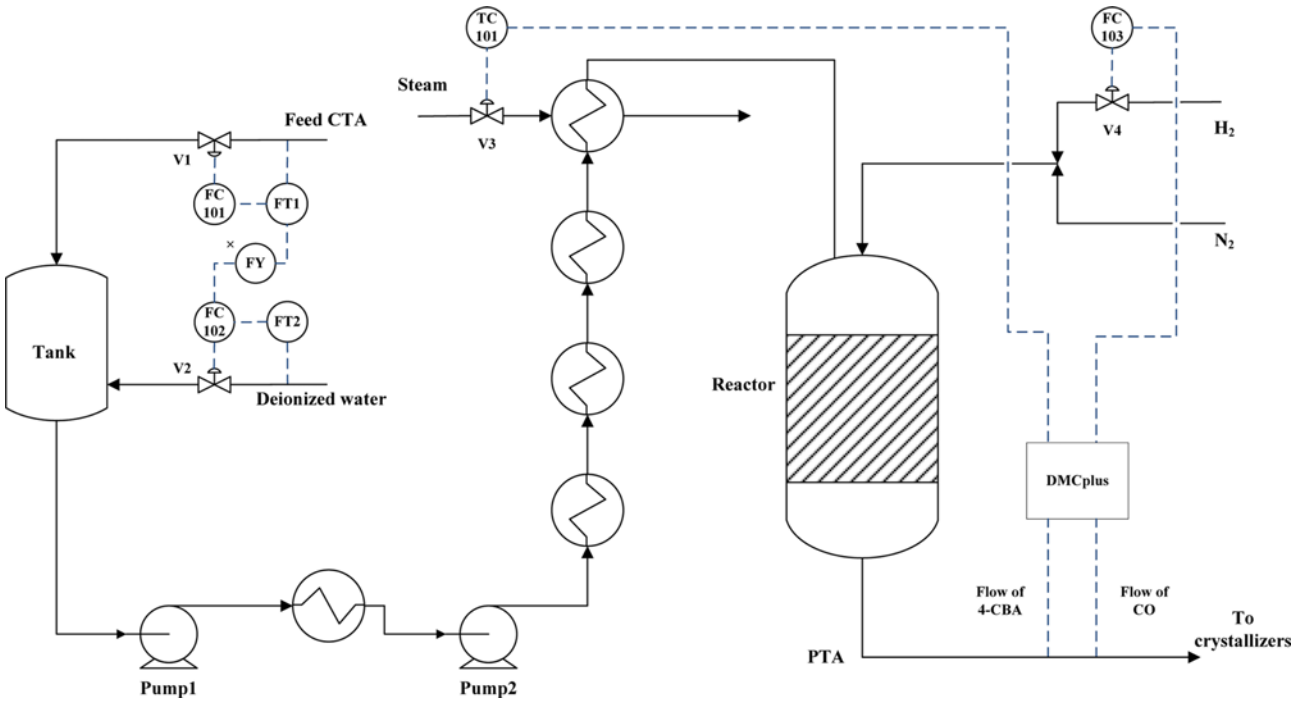

Fig. 12. Control structure of CS4.

of the two PID controllers which control the temperature of the reactor and the flow of H2. In particular, the reactor temperature is determined by the temperature of feed, and for simplicity, the feed temperature is controlled by the flow of steam of the fifth heat exchanger. One PID controller is used to control the flow of steam and the other is used to control the flow of H2. The DMC-PID cascade control system is then accomplished. The development of the entire system is shown in Fig. 11.

2-3. Dynamic Responses of CS3 and CS4

The ±5 mass% step changes in the feed flow of CTA employed in CS2 are the same as the load requirements in CS3 and CS4. Fig. 13 shows the dynamic response of CS3. When the load is decreased by 5%, the process value of FC101 decreases from 80,176.7 kg/hr to 76,167.9 kg/hr, which is similar to that in CS2. When the pressure fluctuates because of the step change, the temperature of the steam decreases to 288.206 °C, eventually increases to 288.29 °C, and then returns to 288.22 °C under the controller TC101. The mass flow of hydrogen initially decreases to 28.99 kg/hr, then increases to 29.176 kg/hr, and finally returns to 29 kg/hr via the controller TC103. The concentration of 4-CBA remains unchanged in the feed CTA, and the mass flow of 4-CBA is reduced. Consequently, the CO discharge of the reactor decreases from 5.255 kg/hr to 5.137 kg/hr, whereas the 4-CBA discharge is reduced to 2.075 kg/hr. The situation is completely different when the load is increased by 5% (Fig. 13). The dynamic responses demonstrate that this strategy cannot effectively control the 4-CBA content and cannot provide a specific value to the flow controller, thereby inducing some difficulties in the industrial process.

The control structure of CS4 is shown in Fig. 12. The response of CS4 is shown in Fig. 14. When the feed flow of CTA decreases by 5%, the flows of 4-CBA and CO in the product are reduced from 2.4 kg/hr to 2.121 kg/hr and from 5.25 kg/hr to 5.01 kg/hr, respectively. The flow of 4-CBA is below the constraint (2.121 kg/hr). Meanwhile, the DMC controller receives the input signals of 4-CBA and CO, and the output signals of DMC controller (the SPRemotes of mass flow of FC103.H2 and TC101.steam) are changed. The flow of hydrogen initially increases from 29 kg/hr to 29.232 kg/hr and then returns to 29 kg/hr, and the value of temperature decreases from 288.22 °C to 287 °C. Given the setpoint changes of the two PID controllers, the flow of 4-CBA increases to 2.255 kg/hr, which is within the constraint. This dynamic response indicates that when the feed flow is reduced, this DMC-PID cascade control system can maintain the flows of 4-CBA and CO within the constraints. In particular, when the time feed flow is reduced by 5%, the flow of 4-CBA can be maintained within the constraints in CS4, only changing the setpoint of TC automatically via the DMC controller. The exact setpoint values of FC and TC are then provided by the DMC controller, which provides better control targets. When the feed flow of CTA increases by 5%, the 4-CBA flow in the product immediately increases from 2.4 kg/hr to 2.674 kg/hr and the CO increases from 5.25 kg/hr up to 5.437 kg/hr, both 4-CBA and CO are beyond the constraints. The DMC controller receives these signals and transforms the output signals into the PID controllers FC103 and TC101, which adjust the valves to control the flows of hydrogen and steam. In CS4, the control system cannot control the 4-CBA and CO by just relying on the setpoint of TC101; the setpoint change of FC must be altered. After the fluctuations, the temperature increases up to 289.37 °C and eventually remains at 289 °C. Meanwhile, the H_2 flow increases to 31.548 kg/hr and remains constant at 31 kg/hr under the controllers TC101 and FC103. When both the reaction temperature and the flow of hydrogen increase, the reaction rate is accelerated. Accordingly, the flows of 4-CBA

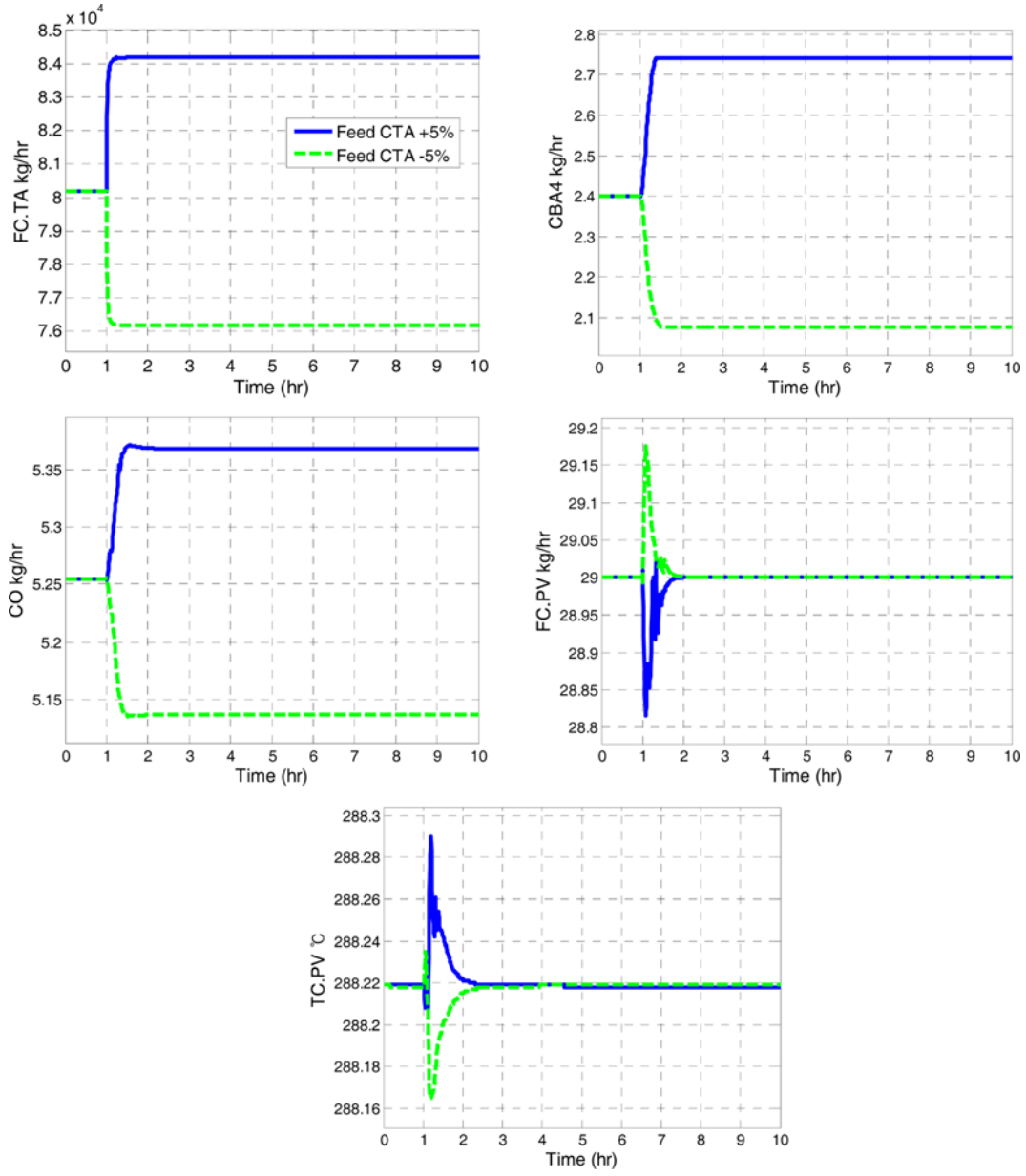

Fig. 13. Dynamic responses of CS3.

and CO decrease from 2.674 kg/hr back to 2.4 kg/hr and 5.437 kg/hr to 5.4 kg/hr, respectively. In this event, both of the two flows are within the constraints. This dynamic response indicates that this DMC-PID cascade control system can maintain the flows of 4-CBA and CO within the constraints when the feed flow of CTA increases by 5%. In particular, the H_2 flow increases to 5.4 kg/hr and the temperature increases to 289 °C when the feed flow of CTA is increased by 5%. Therefore, the DMC-PID cascade control strategy is more effective and accurate in controlling the CTA hydropurification process than the simple-loop PID control strategy.

CONCLUSIONS

We have developed a clearer and more stable dynamic model of CTA hydropurification to simulate the dynamic responses of the industrial process. The kinetic data of the reactions are re-adjusted in the steady-state simulation based on real plant data, and the controller parameters are reset in the dynamic model based on the Tyreus-Luyben settings, resulting in good performance. The advanced control structures in the CTA hydropurification process, a double closed-loop ratio control system and a DMC-PID cascade strategy, are also discussed via the dynamic model, which exhibits better control performance than the traditional control structures.

The control performances demonstrate the following conditions: (1) through the ratio controller, the double closed-loop ratio control system can maintain constant slurry concentration, which is highly needed in CTA hydropurification; (2) the MPC controller can resist disturbances, such as the step change of feed CTA flow,

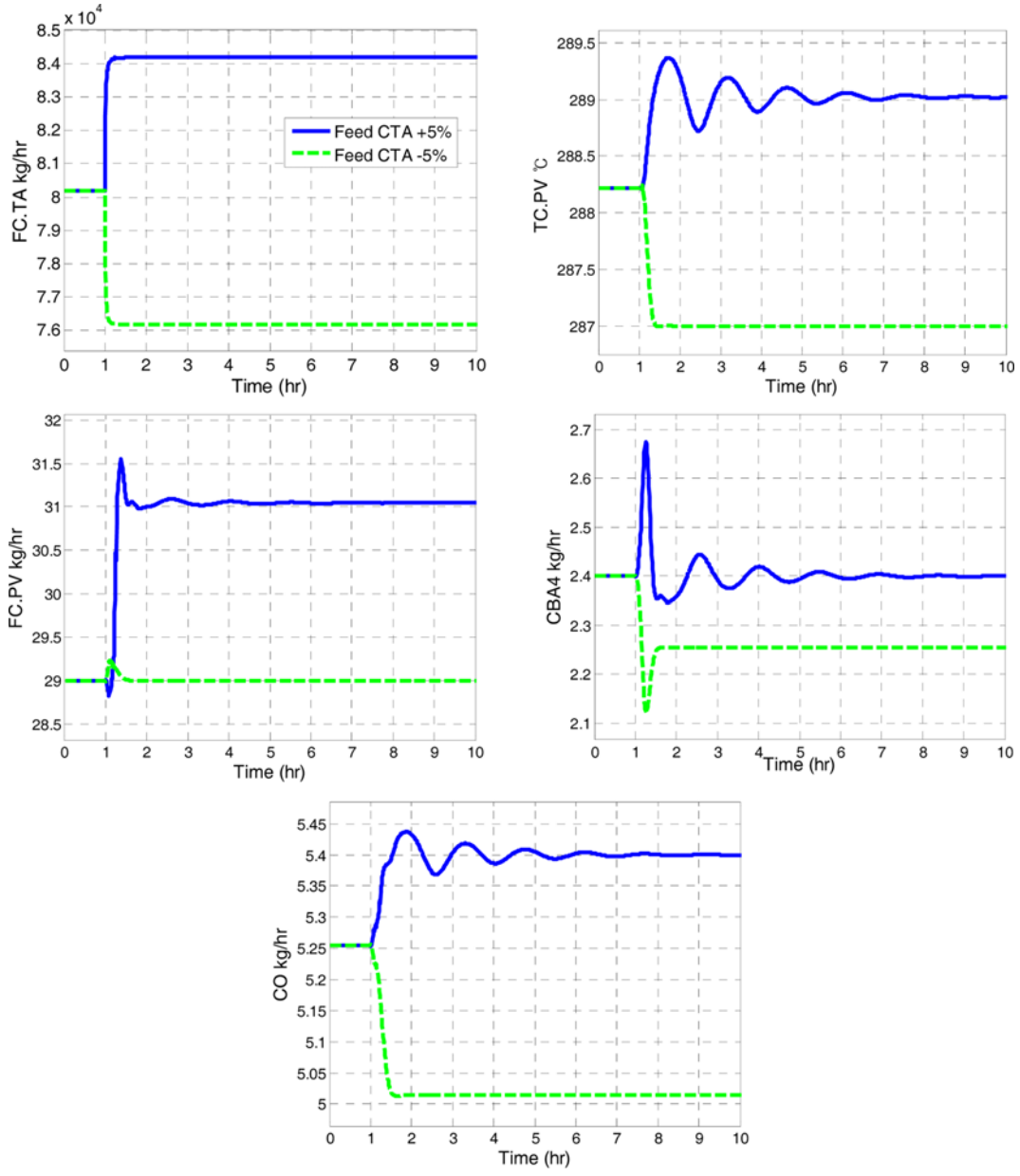

Fig. 14. Dynamic responses of CS4.

and can maintain the key flows of 4-CBA and CO within the constraints. The proposed methods are very prompt and effective in controlling the product quality. The results of this study provide theoretical bases for the advanced control of the CTA hydropurification process.

ACKNOWLEDGEMENT

This study is supported by the Major State Basic Research Development Program of China (2012CB720500), National Natural Science Foundation of China (U1162202, 61174118), Fundamental Research Funds for the Central Universities and Shanghai R&D Platform Construction Program (13DZ2295300), Shanghai Leading Academic Discipline Project (B504), and the State Scholarship Fund of China (CSC:201206745009).

REFERENCES

1. A. Cincotti, A. Orru and G. Cao, *Chem. Eng. Sci.*, **52**, 4205 (1997).
2. R. Burri, K. W. Jun, J. S. Yoo, C. W. Lee and S. E. Park, *Catal. Lett.*, **81**, 169 (2002).
3. S. Jhung, *Korean Chem. Soc.*, **23**, 503 (2002).
4. D. E. James, US Patent, 4,782,181 (1988).
5. H. Köpnick, M. Schmidt, W. Brügging, J. Rüter and W. Kaminsky, *Ullmann's Encyclopedia of Industrial Chemistry*, Wiley (1992).
6. A. Azarpour and G. Zahedi, *Chem. Eng. J.*, **209**, 180 (2012).
7. P. M. Brown and A. S. Myerson, *AIChE J.*, **35**, 1749 (1989).
8. S. Gaines and A. S. Myerson, *AIChE Symp. Ser.*, **78**, 42 (1982).

9. S. Gaines and A. S. Myerson, *Part. Sci. Technol.*, **1**, 409 (1983).
10. S. Zhang, J. Zhou and W. Yuan, *Chem. Reaction Eng. Technol.*, **24**, 54 (2008).
11. J. Xing, Y. Qiao and W. Zhong, *Journal of Hangzhou Dianzi University*, **30**, 55 (2010).
12. W. Zhong, Y. Liu, F. Qian, N. Luo, X. Huang and J. Xing, *Comput. Appl. Chem.*, **29**, 374 (2012).
13. P. Raghavendrachar and S. Ramachandran, *Ind. Eng. Chem. Res.*, **31**, 453 (1992).
14. H. P. Huang, H. Y. Lee and T. K. Gau, *Ind. Eng. Chem. Res.*, **46**, 505 (2007).
15. H. Y. Lee and H. P. Huang, *Ind. Eng. Chem. Res.*, **47**, 3046 (2008).
16. F. Qian, L. Tao, W. Sun and W. Du, *Ind. Eng. Chem. Res.*, **51**, 3229 (2012).
17. S. Li, *Ind. Eng. Chem. Res.*, **48**, 6358 (2009).
18. X. Huang, W. Zhong, W. Du and F. Qian, *Ind. Eng. Chem. Res.*, **52**, 2944 (2013).
19. C. Li, *Chinese J. Chem. Eng.*, **19**, 89 (2011).
20. S. W. Sung, J. Lee and I. B. Lee, *Process Identification and PID Control,* 1st Ed., Wiley (2009).
21. P. Tatjewski, *Advanced Control of Industrial Processes, Structures and Algorithms,* 1st Ed., Springer (2007).
22. J. Richalet, A. Rault, J. L. Testud and J. Papon, *Automatica*, **14**, 413 (1978).
23. D. W. Clarke, C. Mohtadi and P. S. Tuffs, *Automatica*, **23**, 137 (1987).
24. W. L. Luyben, *AIChE J.*, **43**, 12 (1997).
25. W. L. Luyben, *Ind. Eng. Chem. Res.*, **49**, 6150 (2010).
26. W. L. Luyben, *Ind. Eng. Chem. Res.*, **49**, 719 (2010).
27. J. Zhou, T. Zhang and Z. Sui, *Journal of East China University of Science and Technology (Natural Science Edition),* **32**, 374 (2006).
28. J. Zhou, T. Zhang and Z. Sui, *Journal of East China University of Science and Technology (Natural Science Edition)*, **32**, 503 (2006).
29. B. D. Tyreus and W. L. Luyben, *Ind. Eng. Chem. Res.*, **31**, 2625 (1992).
30. Aspen Technology, Inc. *Aspen DMCplus Reference* (2007).